

## Separating positive and negative magnetoresistance for polyaniline-silicon nanocomposites in variable range hopping regime

Hongbo Gu (谷红波),<sup>1,2</sup> Jiang Guo (郭江),<sup>1,3</sup> Rakesh Sadu,<sup>1</sup> Yudong Huang (黄玉东),<sup>2</sup> Neel Haldolaarachchige,<sup>4</sup> Daniel Chen,<sup>1</sup> David P. Young,<sup>4</sup> Suying Wei (魏素英),<sup>3,a)</sup> and Zhanhu Guo (郭战虎)<sup>1,a)</sup>

<sup>1</sup>Integrated Composites Lab (ICL), Dan F. Smith Department of Chemical Engineering, Lamar University, Beaumont, Texas 77710, USA

<sup>2</sup>School of Chemical Engineering and Technology, Harbin Institute of Technology, Harbin 150001, Heilongjiang, China

<sup>3</sup>Department of Chemistry and Biochemistry, Lamar University, Beaumont, Texas 77710, USA

<sup>4</sup>Department of Physics and Astronomy, Louisiana State University, Baton Rouge, Louisiana 70803, USA

(Received 25 February 2013; accepted 9 May 2013; published online 28 May 2013)

This letter reports on unique room temperature organic magnetoresistance (OMAR) in the disordered polyaniline/silicon polymer nanocomposites in the variable range hopping regime. A transition from positive to negative OMAR was observed around 5.5 T. The theoretical analysis revealed that both wave-function shrinkage model and forward interference model contributed to the positive OMAR and only forward interference model was responsible for the observed negative OMAR. The obtained positive OMAR is well explained by the introduced localization length  $a_0$ , density of states at the Fermi level ( $N(E_F)$ ), and average hopping length  $R_{\text{hop}}$ ; and the negative OMAR is interpreted by the quantum interference effect. © 2013 AIP Publishing LLC. [<http://dx.doi.org/10.1063/1.4807787>]

The intrinsic magnetoresistance (MR) (defined as  $MR = (R(H) - R(0))/R(0)$ , where  $R(0)$  is the resistance without magnetic field,  $R(H)$  is the resistance under the magnetic field  $H$ .) observed in an organic semiconductors (OSCs) when a small magnetic field is applied is called organic magnetoresistance (OMAR).<sup>1</sup> This OMAR effect has gained broad interests over the last decade<sup>2,3</sup> due to its potential as the promising spintronic materials and its weak spin-orbit coupling and hyperfine interaction of the carbon element.<sup>3,4</sup> Meanwhile, Mukherjee and Menon<sup>5</sup> have investigated the MR in the doped organic polymer polyaniline (PANI) under high magnetic field, which gives a broader context regarding the OMAR effect. Understanding the mechanisms of OMAR can help the structure design of the organic spintronic devices and develop the future applications.<sup>6</sup> Recently, both positive and negative OMAR have been reported in the OSCs, exhibiting a transition between negative and positive depending on temperature, voltage, and magnetic field.<sup>7</sup> The investigation on the OMAR sign change is important for understanding the origin of OMAR.<sup>6</sup> Jaiswal *et al.*<sup>8</sup> have reported that the MR in the optically transparent single-wall carbon nanotube (SWNT) networks involved the interaction of the forward interference process and shrinkage of electronic wave-function, which lead to the negative MR and positive MR, respectively. Generally, for highly disorderedly localized systems in the variable-range hopping (VRH) regime, both forward interference model and wave-function shrinkage model have been used to describe the observed MR effects (refer to supporting materials, SI).<sup>9,13</sup> The forward interference model can be written as<sup>10</sup>

$$MR = \frac{R(H, T) - R(0, T)}{R(0, T)} \approx -C_{\text{sat}} [H/H_{\text{sat}}] = -C_{\text{sat}} \frac{H}{0.7 \left(\frac{8}{3}\right)^{3/2} \left(\frac{1}{a_0^2}\right) \left(\frac{h}{e}\right) \left(\frac{T}{T_0}\right)^{3/8}}, \quad (1)$$

where the fitting parameter  $C_{\text{sat}}$  is the saturation constant, which represents that the MR value at the effective saturation magnetic field  $H_{\text{sat}}$ ,  $h$  is Planck's constant,  $e$  is electron charge,  $T_0$  is the Mott characteristic temperature, and  $a_0$  is the localization length of the localized wave function of charge carriers. The wave-function shrinkage model can be described as<sup>11</sup>

$$MR = \frac{R(H, T) - R(0, T)}{R(0, T)} \approx t_2 \frac{H^2}{P_C^2} \left(\frac{T_0}{T}\right)^{1/4} = t_2 \frac{e^2 a_0^4}{36 \hbar^2} \left(\frac{T_0}{T}\right)^{3/4} H^2. \quad (2)$$

These two theoretical models are often combined together to explain the MR transition from negative to positive or positive to negative, as expressed<sup>12</sup>

$$MR = -C_{\text{sat}} \frac{H}{0.7 \left(\frac{8}{3}\right)^{3/2} \left(\frac{1}{a_0^2}\right) \left(\frac{h}{e}\right) \left(\frac{T}{T_0}\right)^{3/8}} + t_2 \frac{e^2 a_0^4}{36 \hbar^2} \left(\frac{T_0}{T}\right)^{3/4} H^2. \quad (3)$$

In the forward interference model, the effect of interference among various hopping paths is concerned.<sup>11</sup> Meanwhile, in the wave-function shrinkage model, the contraction of the electronic wave function at impurity centers in the magnetic

<sup>a)</sup> Authors to whom correspondence should be addressed. Electronic addresses: [suying.wei@lamar.edu](mailto:suying.wei@lamar.edu) and [zhanhu.guo@lamar.edu](mailto:zhanhu.guo@lamar.edu)

field leads to a reduction in the hopping length between two sites and causes a positive MR.<sup>11</sup> Although Bloom *et al.*<sup>6</sup> have used bipolaron model to separate the positive and negative MR contributions in the tris-(8 hydroxyquinolino) aluminum (Alq<sub>3</sub>, C<sub>27</sub>H<sub>18</sub>N<sub>3</sub>O<sub>3</sub>Al) system by assuming that the total MR is a superposition of the positive and negative MR effects using the empirical law of non-Lorentzian line shape, the separation of positive and negative MR in the conductive polymer systems using forward interference model and wave-function shrinkage model has not been reported so far.

In this letter, we report on the separation of room temperature positive and negative MR in disordered conductive polymer nanocomposites (PNCs) consisting of silicon (10 wt. %)/PANI in the VRH regime by forward interference model and wave-function shrinkage model. The detailed information about the preparation of silicon/PANI PNCs using a surface initiated polymerization (SIP) method is provided in the supporting information, SI.<sup>13</sup> The resistivity ( $\rho$ ) was measured by a standard four-probe method from 100 to 290 K. The sample was prepared by pressing silicon/PANI PNC powders into disc pellet form with a diameter of 25 mm by applying a pressure of 50 MPa in a hydraulic presser and the average thickness was about 1.0 mm. The temperature dependent resistivity was used to determine the electrical conduction mechanism in the silicon/PANI PNCs. The same sample was used for MR measurements, which were carried out using a standard four-probe technique by a 9-T Physical Properties Measurement System (PPMS) by Quantum Design at room temperature. The four probes were 0.002 in. diameter platinum wires, which were attached by silver paste to the sample. And the magnetic field was applied perpendicular to the sample.

The temperature dependent resistivity for the silicon/PANI PNCs is shown in Fig. 1(a). The electrical conduction mechanism is illustrated via the obtained temperature dependent resistivity using Mott VRH approach, which describes the low temperature resistivity in the strongly disordered systems at the localized states and is expressed as<sup>14</sup>

$$\sigma = \sigma_0 \exp \left[ - \left( \frac{T_0}{T} \right)^{\frac{1}{n+1}} \right], \quad (4)$$

where the constant  $\sigma_0$  stands for the conductivity at infinite low temperature,  $T$  (K) is the Kelvin temperature, and

constant  $T_0$  (K) is the Mott characteristic temperature and expressed as<sup>15</sup>

$$T_0 = 24 / [\pi k_B N(E_F) a_0^3], \quad (5)$$

where  $a_0$  is the localization length,  $k_B$  is Boltzmann constant, and  $N(E_F)$  is the density of states at the Fermi level. From Eq. (5), the  $T_0$  is noticed to be inversely proportional to the  $a_0^3$ , which indicates that the higher  $T_0$ , the stronger charge carriers scattering and the higher resistivity.<sup>16</sup> The value  $n$  is the dimension of the system and  $n = 3, 2,$  and  $1$  stands for 3-, 2-, and 1-dimensional systems, respectively.<sup>17</sup> The  $\sigma_0$  and  $T_0$  could be obtained from the intercept and slope of the linear fitting  $\ln(\sigma) \sim T^{-1/(n+1)}$ . The best linear fits of  $\ln(\sigma) \sim T^{-1/(n+1)}$  for the silicon/PANI PNCs obtained from Fig. 1(a) is shown in Fig. 1(b) with  $n = 3$  in the temperature range of 100–290 K, indicating that the synthesized PNCs obey a quasi 3-d VRH electrical conduction mechanism. The calculated  $\sigma_0$  and  $T_0$  are  $2.70 \times 10^5 \text{ S cm}^{-1}$  and  $2.67 \times 10^7 \text{ K}$ , respectively.

The room temperature MR result for the synthesized PNCs calculated from  $MR = (R(H) - R(0))/R(0)$  is shown in Fig. 2(a). A MR value transition from positive to negative is observed at around 5.5 T in the PNCs. As aforementioned, these disordered silicon/PANI PNCs follow a quasi 3-d VRH mechanism and thus Eq. (3) is proper to formulate this MR transition with the assistance of POLYMATH software. Both the forward interference model and the wave-function shrinkage model are observed to contribute to the positive MR part, and the fitting graph is shown in Fig. 2(b) with a fitting correlation coefficient  $R^2$  of 0.9998144. The obtained fitting parameter  $C_{\text{sat}}$  is  $2.345 \times 10^{-4}$  and thus the measured positive room temperature MR in these PNCs can be expressed as

$$MR = -2.345 \times 10^{-4} \times \frac{H}{0.7 \left( \frac{8}{3} \right)^{3/2} \left( \frac{1}{a_0^2} \right) \left( \frac{h}{e} \right) \left( \frac{T}{T_0} \right)^{3/8}} + t_2 \frac{e^2 a_0^4}{36 \hbar^2} \left( \frac{T_0}{T} \right)^{3/4} H^2. \quad (6)$$

Meanwhile, it is worthy to mention that only the forward interference model contributes to the negative MR part and the fitting correlation coefficient  $R^2$  is 0.9999959. The obtained fitting graph is displayed in Fig. 2(c) and the measured negative room temperature MR in these PNCs can be described as

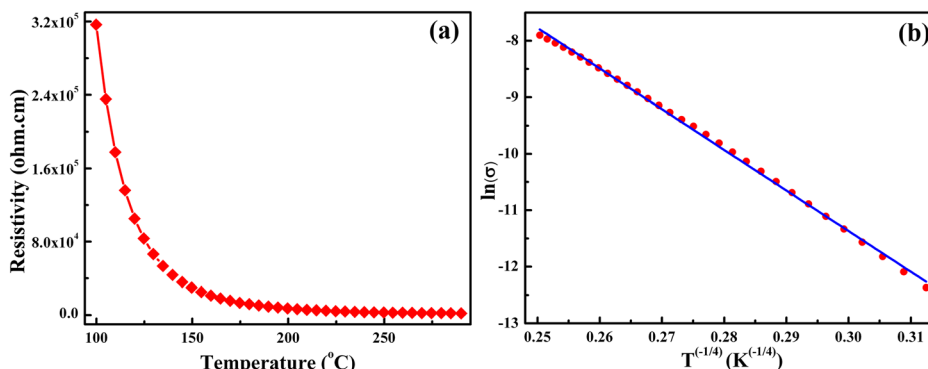


FIG. 1. (a) Resistivity vs. temperature for the silicon/PANI PNCs; and (b)  $\ln(\sigma)$  and  $T^{-1/4}$  curve for silicon/PANI PNCs.

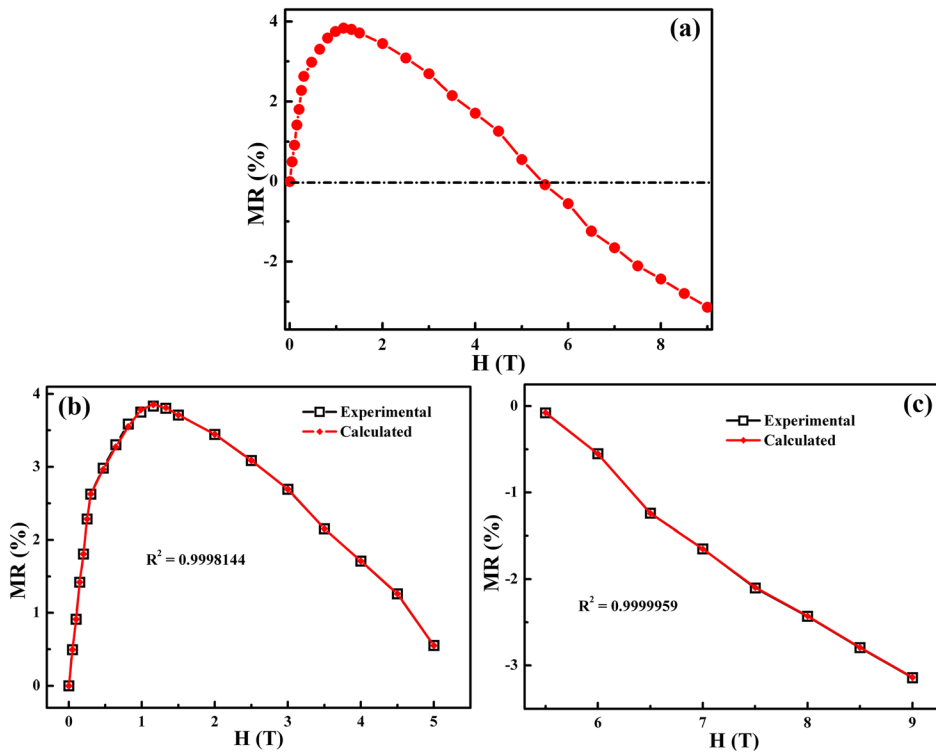


FIG. 2. (a) Experimental measured room temperature MR, (b) calculated MR of the silicon/PANI PNCs ( $H < 5\text{ T}$ ), and (c) calculated MR of the silicon/PANI PNCs ( $H > 5\text{ T}$ ).

$$MR = -2.345 \times 10^{-4} \times \frac{H}{0.7 \left(\frac{8}{3}\right)^{3/2} \left(\frac{1}{a_0^2}\right) \left(\frac{h}{e}\right) \left(\frac{T}{T_0}\right)^{3/8}} \quad (7)$$

The calculated localization length  $a_0$  through fitting with POLYMATH software is listed in Table I. The  $a_0$  value decreases with increasing magnetic field at the positive MR part ( $H < 5.5\text{ T}$ ), which corresponds to the wave-function shrinkage. After the MR switches from positive to negative, the  $a_0$  increases dramatically with increasing magnetic field, indicating that the wave function shrinkage effect does not exist at all. Only the forward interference model can explain the observed negative MR. From the obtained fitting results, the MR signal of the disordered silicon/PANI PNCs can be separated into two parts: positive signal and negative signal. The positive signal is depicted in following equation and shown in Fig. 3(a):

$$MR^+ = t_2 \frac{e^2 a_0^4}{36 \hbar^2} \left(\frac{T_0}{T}\right)^{3/4} H^2 \quad (H < 5.5\text{ T}). \quad (8)$$

The negative signal can be calculated from the following equation and shown in Fig. 3(b):

$$MR^- = -2.345 \times 10^{-4} \times \frac{H}{0.7 \left(\frac{8}{3}\right)^{3/2} \left(\frac{1}{a_0^2}\right) \left(\frac{h}{e}\right) \left(\frac{T}{T_0}\right)^{3/8}} \quad (9)$$

These results indicate that the MR in the disordered silicon/PANI PNCs system is strongly magnetic field dependent and obeys different models with the change of magnetic field. The density of states at the Fermi level  $N(E_F)$  can be calculated from the following equation and the obtained  $a_0$ :

$$N(E_F) = 24 / [\pi k_B T_0 a_0^3]. \quad (10)$$

The corresponding calculated  $N(E_F)$  is also listed in Table I. Generally, the hopping probability between the localized states increases with increasing  $N(E_F)$ ,<sup>19</sup> which means the higher the  $N(E_F)$ , the higher the hopping probability. A higher hopping probability also corresponds to a shorter  $a_0$ .

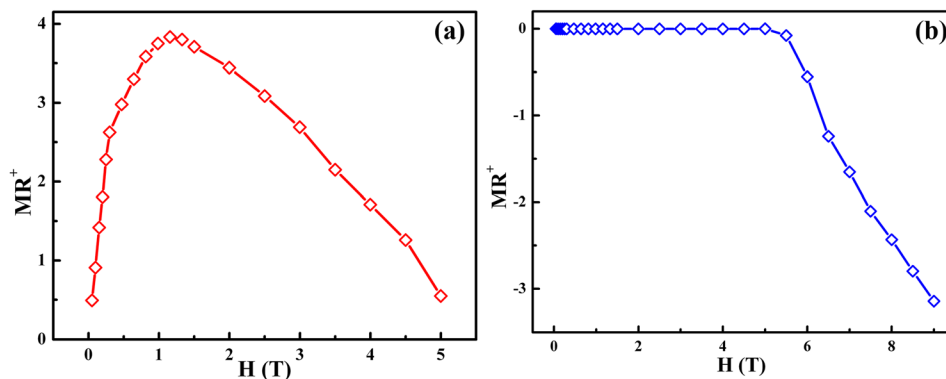


FIG. 3. (a)  $MR^+$  obtained from wave-function shrinkage model; (b)  $MR^-$  obtained from forward interference model.

TABLE I. Calculated localization length  $a_0$ ,  $N(E_F)$ , and  $R_{\text{hop}}$  for the silicon/PANI PNCs.

Parameter	Magnetic field (T)						
	0.10	0.30	1.16	3.00	5.00	5.50	9.00
$a_0$ (nm)	102.05	76.76	42.96	24.42	12.72	102.47	507.97
$N(E_F)$ ( $\text{J}^{-1} \text{cm}^{-3}$ )	$1.95 \times 10^{31}$	$4.58 \times 10^{31}$	$2.61 \times 10^{32}$	$1.42 \times 10^{33}$	$1.00 \times 10^{34}$	$1.93 \times 10^{31}$	$1.58 \times 10^{29}$
$R_{\text{hop}}$ (nm)	666.61	501.40	280.64	159.55	83.09	669.36	3318.13

From Table I,  $a_0$  is observed to decrease as magnetic field increase to 5 T, after that  $a_0$  increases with increasing magnetic field. The  $N(E_F)$  shows the opposite trend to  $a_0$ , which means that the hopping probability increases with increasing magnetic field ( $H < 5$  T) and then decreases.

The average hopping length,  $R_{\text{hop}}$ , can be obtained from the following equation:<sup>20</sup>

$$R_{\text{hop}} = (3/8)(T_0/T)^{1/4}a_0. \quad (11)$$

The calculated  $R_{\text{hop}}$  (nm) is shown in Table I, which indicates a magnetic field dependent  $R_{\text{hop}}$  behavior. Normally, the positive MR in the hopping system is due to the charge carrier hopping conduction arising from the contraction of the charge carrier wave function and the subsequent reduced  $R_{\text{hop}}$ .<sup>14</sup> From the results listed in Table I, the  $R_{\text{hop}}$  for the positive MR is observed to decrease significantly as the MR reaches the peak and then decreases slightly. The more reduced  $R_{\text{hop}}$ , the higher MR is obtained. However, for the negative MR, the  $R_{\text{hop}}$  increases dramatically with increasing magnetic field. In fact, the wave function shrinkage effect is not valid in the negative MR due to the much larger  $a_0$  and  $R_{\text{hop}}$ ; therefore, the term of quantum interference effect is introduced to explain the negative MR, which is also observed in the bulk samples of single walled carbon nanotubes.<sup>21</sup> The calculated  $a_0$ ,  $N(E_F)$ , and  $R_{\text{hop}}$  for the silicon/PANI PNCs at different magnetic fields are listed in Table SI.<sup>13</sup>

In conclusion, the disordered conductive silicon/PANI PNCs have been demonstrated to follow variable range hopping regime by the temperature dependent resistivity study. The observed switching MR from positive at low magnetic field to negative at high magnetic field has been explained by the forward interference model and wave-function shrinkage model via POLYMATH software. Both models contribute to the positive part in the obtained OMAR signal and only the forward interference model is devoted to the negative part of OMAR effect. The obtained positive MR is well explained by the introduced  $a_0$ ,  $N(E_F)$ , and  $R_{\text{hop}}$ ; and negative MR is interpreted by the quantum interference effect.

This project was financially supported by Research Enhancement Grant (REG) of Lamar University and the National Science Foundation Nanoscale Interdisciplinary Research Team, and Materials Processing and Manufacturing (CMMI 10-30755). D. P. Young acknowledges support from the National Science Foundation under

Grant No. DMR 10-05764. H. Gu acknowledges the support from China Scholarship Council (CSC) program.

<sup>1</sup>F. L. Bloom, M. Kemerink, W. Wagemans, and B. Koopmans, *Phys. Rev. Lett.* **103**(6), 066601 (2009); T. L. Francis, Ö. Mermer, G. Veeraghavan, and M. Wohlgenannt, *New J. Phys.* **6**(1), 185 (2004).

<sup>2</sup>V. Dediu, M. Murgia, F. C. Matocota, C. Taliani, and S. Barbanera, *Solid State Commun.* **122**(3–4), 181 (2002); H. Gu, Y. Huang, X. Zhang, Q. Wang, J. Zhu, L. Shao, N. Haldolaarachchige, D. P. Young, S. Wei, and Z. Guo, *Polymer* **53**(3), 801 (2012); H. Gu, X. Zhang, H. Wei, Y. Huang, S. Wei, and Z. Guo, *Chem. Soc. Rev.* DOI: 10.1039/C3CS60074B (published online).

<sup>3</sup>I. Bergenti, V. Dediu, M. Prezioso, and A. Riminucci, *Philos. Trans. R. Soc. London, Ser. A* **369**(1948), 3054 (2011).

<sup>4</sup>V. Alek Dediu, L. E. Hueso, I. Bergenti, and C. Taliani, *Nature Mater.* **8**(9), 707 (2009).

<sup>5</sup>A. K. Mukherjee and R. Menon, *J. Phys. Condens. Matter* **17**(12), 1947 (2005).

<sup>6</sup>F. L. Bloom, W. Wagemans, M. Kemerink, and B. Koopmans, *Phys. Rev. Lett.* **99**(25), 257201 (2007).

<sup>7</sup>J. C. Clark, G. G. Ihas, A. J. Rafanello, M. W. Meisel, M. Reghu, C. O. Yoon, Y. Cao, and A. J. Heeger, *Synth. Met.* **69**(1–3), 215 (1995); Ö. Mermer, G. Veeraghavan, T. L. Francis, Y. Sheng, D. T. Nguyen, M. Wohlgenannt, A. Köhler, M. K. Al-Suti, and M. S. Khan, *Phys. Rev. B* **72**(20), 205202 (2005); B. Hu and Y. Wu, *Nature Mater.* **6**(12), 985 (2007).

<sup>8</sup>M. Jaiswal, W. Wang, K. A. Shiral Fernando, Y. Sun, and R. Menon, *Phys. Rev. B* **76**(11), 113401 (2007).

<sup>9</sup>A. Sarkar, P. Ghosh, A. K. Meikap, S. K. Chattopadhyay, S. K. Chatterjee, and M. Ghosh, *Solid State Commun.* **143**(6–7), 358 (2007).

<sup>10</sup>R. Rosenbaum, A. Milner, S. Hannahs, T. Murphy, E. Palm, and B. Brandt, *Physica B* **294–295**, 340 (2001).

<sup>11</sup>T.-I. Su, C.-R. Wang, S.-T. Lin, and R. Rosenbaum, *Phys. Rev. B* **66**(5), 054438 (2002).

<sup>12</sup>R. Rosenbaum, A. Milner, R. Haberkern, P. Häussler, E. Palm, T. Murphy, S. Hannahs, and B. Brandt, *J. Phys. Condens. Matter* **13**(13), 3169 (2001).

<sup>13</sup>See supplementary material at <http://dx.doi.org/10.1063/1.4807787> for detail description of forward interference model and wave-function shrinkage model; preparation of silicon/PANI nanocomposites; and for calculated  $a_0$ ,  $N(E_F)$ , and  $R_{\text{hop}}$  at different magnetic fields.

<sup>14</sup>J. Zhu, H. Gu, Z. Luo, N. Haldolaarachchige, D. P. Young, S. Wei, and Z. Guo, *Langmuir* **28**, 10246 (2012).

<sup>15</sup>J. Guo, H. Gu, H. Wei, Q. Zhang, N. S. Haldolaarachchige, Y. Li, D. P. Young, S. Wei, and Z. Guo, *J. Phys. Chem. C* **117**(19), 10191–10202 (2013).

<sup>16</sup>H. Gu, J. Guo, X. Zhang, Q. He, Y. Huang, H. A. Colorado, N. S. Haldolaarachchige, H. L. Xin, D. P. Young, S. Wei, and Z. Guo, *J. Phys. Chem. C* **117**(12), 6426 (2013).

<sup>17</sup>Z. Guo, K. Shin, A. Karki, D. P. Young, R. Kaner, and H. Hahn, *J. Nanopart. Res.* **11**, 1441 (2009).

<sup>18</sup>H. Gu, J. Guo, H. We, Y. Huang, C. Zhao, Y. Li, Q. Wu, N. Haldolaarachchige, D. P. Young, S. Wei, and Z. Guo, *Phys. Chem. Chem. Phys.* DOI: 10.1039/C3CP50698C (published online).

<sup>19</sup>K. Dutta and S. K. De, *Phys. Lett. A* **361**, 141 (2007).

<sup>20</sup>Y. Long, Z. Chen, X. Zhang, J. Zhang, and Z. Liu, *Appl. Phys. Lett.* **85**, 1796 (2004).

<sup>21</sup>Y. Yosida and I. Oguro, *J. Appl. Phys.* **86**, 999 (1999).